



HHS Public Access

Author manuscript

Acta Biomater. Author manuscript; available in PMC 2018 January 27.

Published in final edited form as:

Acta Biomater. 2016 October 01; 43: 327–337. doi:10.1016/j.actbio.2016.07.051.

Biomimetic Hydrogel with Tunable Mechanical Properties for Vitreous Substitutes

Sruthi Santhanam^b, Jue Liang^a, Jessica Struckhoff^{a,c}, Paul D. Hamilton^a, and Nathan Ravi^{a,b,c,*}

^aDepartment of Ophthalmology and Visual Science, Washington University School of Medicine, MO

^bEnergy, Environmental and Chemical Engineering, Washington University in St Louis, MO

^cDepartment of Veterans Affairs St Louis Medical Center, St Louis, MO

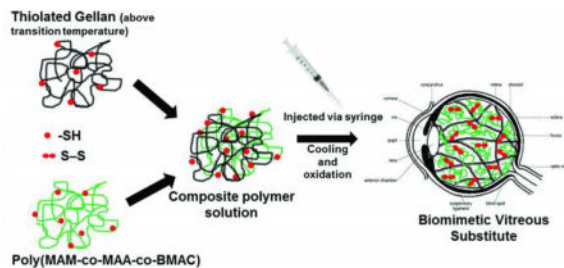
Abstract

The vitreous humor of the eye is a biological hydrogel principally composed of collagen fibers interspersed with hyaluronic acid. Certain pathological conditions necessitate its removal and replacement. Current substitutes, like silicone oils and perfluorocarbons, are not biomimetic and have known complications. In this study, we have developed an *in situ* forming two-component biomimetic hydrogel with tunable mechanical and osmotic properties. The components are gellan, an analogue of collagen, and poly(methacrylamide-co-methacrylate), an analogue of hyaluronic acid; both endowed with thiol side groups. We used response surface methodology to consider seventeen possible hydrogels to determine how each component affects the optical, mechanical, sol-gel transition temperature and swelling properties. The optical and physical properties of the hydrogels were similar to vitreous. The shear storage moduli ranged from 3 to 358 Pa at 1Hz and sol-gel transition temperatures from 35.5 to 43 °C. The hydrogel had the ability to remain swollen without degradation for four weeks *in vitro*. Three hydrogels were tested for biocompatibility on primary porcine retinal pigment epithelial cells, human retinal pigment epithelial cells, and fibroblast (3T3/NIH) cells, by electric cell-substrate impedance sensing system. The two-component hydrogels allowed for the tuning and optimizing of mechanical, swelling, and transition temperature to obtain three biocompatible hydrogels with properties similar to vitreous. Future studies include testing of the optimized hydrogels in animal models for use as a long-term substitute, whose preliminary results are mentioned.

Graphical abstract

Correspondence to: Nathan Ravi, Department of Ophthalmology and Visual Sciences, Washington University in St. Louis; 660, South Euclid, Campus box 8096, St. Louis 63110, USA. Tel.: +1 314-747-4458; fax: +1 314 -747-5073; ravi@vision.wustl.edu.

Publisher's Disclaimer: This is a PDF file of an unedited manuscript that has been accepted for publication. As a service to our customers we are providing this early version of the manuscript. The manuscript will undergo copyediting, typesetting, and review of the resulting proof before it is published in its final citable form. Please note that during the production process errors may be discovered which could affect the content, and all legal disclaimers that apply to the journal pertain.



Keywords

Biomimetic; hydrogels; *in situ* gelation; biocompatibility; vitreous

1. Introduction

Vitreous humor is a clear, jelly-like structure that occupies two-thirds of the posterior segment of the human eye (by volume) [1]. It is transparent to visual light, has a refractive index (RI) of 1.3345–1.3348 and has a density of 1.0053–1.0089. It is a virtually acellular, highly hydrated, extracellular gel matrix primarily composed of bound and free water, with less than 1% (w) of collagen and hyaluronic acid (HA). Collagen (type II) is an abundant vitreous structural protein with a rigid-rod-like triple helix structure that forms scaffold-like network in the vitreous. HA is a disaccharide polymer with a randomly coiled structure in solution, which stabilizes the collagen network, exerts an osmotic pressure that holds the retina in its position [2]. Collagen and HA form an interpenetrating network that behaves as a viscoelastic solid [3] and acts as a shock absorber, dampening the intra-ocular motions and vibrations. Ocular trauma and various ocular diseases require the removal of vitreous gel that is replaced with a substitute. Air, balanced salt solutions, perfluorocarbons (PFC), expansile gases, and silicone oils are used as replacements based on the clinical need [4]. Expansile PFC gases are used as short-term substitutes for post-operative endo-tamponade and PFC liquids as intra-surgery tool to temporarily flatten the retina, which are exchanged for long-term substitutes. Silicone oil is clinically accepted for short- or long-term tamponade to treat complex retinal detachments. However, there are various limitations with each substitute such as expansion of gases at high altitudes, the toxic nature of PFCs, elevated intraocular pressure, and lipophilic nature, emulsification and post-vitreotomic complications, particularly with the use of silicone oil, which requires a second surgery for its removal [5–7]. In addition, current vitreous substitutes that work by surface tension and pneumatic pressure to hold the retina in its position alter the refractive error of the eye, and cause significant patient burden. Hence, there is a need for long-term vitreous substitute. Our approach is to develop an *in situ* forming substitute that mimics the natural vitreous and in the process, enables us to gain more insight into the structure and physiology of the natural vitreous. Furthermore, a biomimetic gel will expand our knowledge of the role of the vitreous structure and its relation to its properties.

Several *in situ* forming hydrogels have been proposed as vitreous substitutes, including HA [8, 9], polyvinylalcohol [10], polyethylene glycol [11–13], and polyacrylamide (PAM) [14, 15]. An *in situ* forming hydrogel has several substantial benefits other than the physical and

optical properties similar to native vitreous; it is easily injected into the vitreous cavity without any modification of the current vitrectomy procedure, and it does not shear degrade during the injection, a process which causes fragmentation of the pre-formed gel and introduces free radicals into the cavity. Our laboratory has achieved a reversible *in situ* forming PAM hydrogel using thiol cross-linker, which holds potential as a long-term vitreous substitute [15]. The thiol groups in polymer chains, upon oxidation, establish disulfide bonds that can be reduced back to thiols by dithiothreitol (DTT) *ex vivo* or with glutathione *in vivo*. The reversibility potentially eliminates the need for a second surgery in case the hydrogel needs to be removed.

The current work significantly extends our previous work on the use of co-polyacrylamide [15]. Here, we reverse-engineered the critical elements of the natural vitreous (collagen and HA) and consequently have focused on the development of a two-component (rigid and random coil) *in situ* forming hydrogel that mimics the natural vitreous with tunable osmotic/swelling pressure and other mechanical properties. The rigid component of our hydrogel, Gellan, is a bio-polysaccharide, which undergoes sol-gel transition at certain temperature and forms a physical gel almost instantaneously. This transition also occurs in the presence of mono/divalent cations. It is a stiff-biopolymer that has helical conformation at low temperature and swells minimally, analogues to collagen. In addition, it is used in ophthalmic applications [8, 16]. On the other hand, the poly(methacrylamide-co-methacrylate-co-*N,N'*-bis(methylacryloyl-cystamine)) (poly(MAM-co-MAA-co-BMAC)) is a random coil, ionic polyelectrolyte, that allows for variation in the swelling (osmotic pressure) and gelling properties of the hydrogels [17], analogues to HA at a mesoscopic level. Nakagawa [18] observed that a simple combination of collagen and HA does not last long as a vitreous substitute as they diffuse out of the vitreous cavity. To overcome this obstacle, we modified the components of our hydrogel by introducing thiol (-SH) side groups that can form chemical cross-links (S-S) upon physiological oxidation. Our polymer solution can be safely and easily injected into the vitreous cavity at 42 °C that will rapidly form a physically-crosslinked hydrogel instantaneously as it cools to body temperature. The thiol groups will oxidize over time to form a reversible chemically crosslinked *in situ* forming hydrogel capable of generating osmotic pressure to keep the retina in its position (Fig. 1). In addition, the properties of the hydrogel are tunable with change in concentration of each component. To ascertain the composition of this two-component hydrogel that can mimic the properties of natural vitreous, we evaluated the mechanical, optical, physical, transition temperature, swelling and biocompatible properties of a series of statistically designed (Response surface methodology, RSM) hydrogels.

2. Materials and methods

2.1. Materials

Reagents were purchased from Sigma Aldrich Co. (St Louis, MO) and used as received unless otherwise stated. MAA (99%) was purchased from Sigma Aldrich Co. (St Louis, MO) and vacuum distilled before using. Glycine (tissue culture grade) and ethylenediaminetetraacetic acid disodium salt (EDTA, electrophoresis grade) were purchased from Fisher Scientific (Pittsburg, PA) and used as received. Human retinal

pigment epithelial cells (ARPE-19) and 3T3/NIH cell lines were purchased from American Type Culture Collection (Manassas, VA).

2.2. Thiolation of Gellan

A stock aqueous solution of gellan 1.33% (w/v) was prepared by dissolving required quantity of gellan (4 g, 6.2 meq of COOH) in 300 mL of water at 70 °C. The pH of the gellan solution was adjusted to 4.5 and was cooled to 50 °C. 1-Ethyl-3-(3-dimethylaminopropyl) carbodiimide (EDC; 0.76 g, 4.0 mmol), N-hydroxysuccinimide (NHS; 0.26 g, 2.2 mmol) and cystamine dihydrochloride (Cys; 0.70 g, 6.2 mmol) were dissolved in 100 mL of water, and this solution was added to the gellan solution at 50 °C with stirring. The reaction mixture was continuously stirred and was cooled to room temperature in 30 minutes. The mixture formed a gel at room temperature and was allowed to react for four more hours. Thereafter, the reaction was terminated by adjusting the final pH to 8–9. The excess EDC, NHS and Cys were removed from the reaction mixture by dialysis (MWCO: 6000–8000) in de-ionized (DI) H₂O (three times). Then, the pH of the mixture was adjusted to 7.5 and the disulfide bonds were reduced with 5 molar excess of DTT for 3 hours yielding a solution. The excess DTT was removed by dialysis in N₂-bubbled 1 mM HCl (4 L, six times). Finally, the samples were analyzed for the degree of thiolation of gellan by 2-nitro-5-thiosulfobenzonate (NTSB) assay [19].

2.3. Synthesis of poly(MAM-co-MAA-co-BMAC)

The poly (MAM-co-MAA-co-BMAC) (CoP) was synthesized by free radical polymerization of MAM, MAA and BMAC as described in detail by Liang et al. [17]. The disulfide and thiol content in the copolymer was determined by the NTSB assay as used for gellan.

2.4. Response Surface Method Design (RSM)

We used D-Optimal design of RSM (Design-Expert software, version 7, Stat-Ease, Minneapolis, MN) with additional center points and replicates, to observe the relationship between the variables that govern the experiment and one or more responses. The concentrations of thiolated gellan and poly(MAM-co-MAA-co-BMAC) were the two variables. The variables were at five different concentrations with two replicates at each vertex of the design space and three replicates for the center point, resulting in 17 hydrogels with 11 formulations as shown in Table 1 and Fig. A.1. Each formulation was characterized for storage modulus, loss modulus, refractive index, optical transmittance, density, sol-gel transition temperature and degree of swelling.

The formulations of hydrogel were optimized for a refractive index of 1.334–1.338, density of 1.002–1.009, optical transmittance greater than 85% in the visible wavelength, storage moduli of 100–200 Pa, and transition temperature of 38–41°C. The three optimized formulations were used for further *in vitro* biocompatibility studies.

2.5. Synthesis of Composite Hydrogel

Thiolated gellan and poly(MAM-co-MAA-co-BMAC) were dissolved separately according to the required concentration (Table 1) in N₂-bubbled water and their pH was adjusted to 7. About 10% (v/v) of 10× Dulbecco's phosphate buffered saline (PBS) and 1% (v/v) of

antibiotic/antimicrobial solution for the volume of final composite solution was added to the copolymer solution. Both the solutions were heated to 55 °C for 15 minutes separately and finally mixed for investigating the sol-gel transition temperature. Three mL of the composite solution was cast in a pre-weighed sterile 35-mm dish for rheological studies and additional 3 mL was injected into a dialysis cassette (Slice-A-Lyzer, MWCO – 10 kDa, Thermo Scientific, Rockford, IL) for swelling studies. The composite solution was oxidized for a week at 37 °C in a humidified chamber to form a S-S crosslinked composite hydrogel. The gelling of the composite solution was confirmed by tilting the dishes at 45° and observing the resistance to flow. After ensuring that the solution has gelled, PBS (-Ca, -Mg) was added to the dishes containing hydrogels, and gels were left at 37 °C for an additional 7 days to reach equilibrium swelling. Equilibrium swelling was achieved when there was no more increase in weight of the hydrogel.

2.6. Rheological Measurements of Hydrogel

2.6.1. Sol-gel transition temperature—The sol-gel transition characteristic of each formulation of hydrogel was carried out using a Vilastic-3 oscillatory tube rheometer (Vilastic Scientific Inc., Austin, TX). A thermal scan with 5% constant shear strain and 1.0 Hz constant frequency was used to measure the transition point of the hydrogel by cooling the samples from 55 °C to 15 °C, equilibrating within 0.1 °C at each point as described [20]. A 3× molar excess of glutathione was added to the samples during measurement to prevent disulfide cross-linking.

2.6.2. Storage Modulus—To determine the shear storage modulus, frequency scans were performed for the hydrogels at 37 °C using a modular compact rheometer (MCR rheometer; Anton Paar, TX, USA). The excess PBS (-Ca, -Mg) from the swollen hydrogel in 35 mm dishes were removed prior to testing. The hydrogel in the 35 mm dishes were cut with a custom-made cutter of 21 mm diameter. The dishes with 21 mm diameter hydrogel were placed on the plate of the rheometer and were in contact with the measuring system (20 mm plate). A small force (0.2 N) was applied to the gel to ensure good contact. The sample was measured at a 2% strain and constant temperature of 37 °C in a range of frequencies.

2.6.3. Swelling Studies—The hydrogel in dialysis cassettes were swollen in a 1× PBS bathing solution, which was kept in a humidifier chamber at 37 °C for two weeks. The change in weight of the hydrogels before and after the addition of 1× PBS was recorded. The change in swelling of hydrogel in the presence of 1× PBS from its initial was calculated using the formula:

$$\Delta Swelling[\%]=\left(\frac{W_s - W_i}{W_i}\right) * 100$$

Where W_s is the weight of the swollen hydrogel and W_i is the initial weight of the hydrogel

2.7. Physical Properties of Hydrogel

2.7.1. Refractive Index—The refractive index of optimized formulations of hydrogel was determined in an Abbe refractometer (ATAGO Abbe Refractometer NAR-1T, Kirkland, WA). The temperature of the testing was kept at 37 °C at 552 nm.

2.7.2. Optical Transmittance—A UV/VIS spectrophotometer (DU800; BeckmanCoulter Inc., Brea, CA) was used to measure the transmittance of light (280–800 nm) at 25 °C.

2.7.3. Density—The accurate weight of 100 µL of the hydrogel at 25 °C was determined. The weight of 100 µL of water and its density at 25 °C was used as the reference to find the density of the hydrogel.

2.8. Degradation Studies

The degradation study of the hydrogel was carried out *in vitro* by incubating the gel in 1× PBS containing (i) 10,000 U/mL of lysozyme and (ii) 1,000 U/mL of trypsin, separately at 37°C for 4 weeks. Two mL of lysozyme and trypsin solution was added to the pre-weighed 35 mm dishes containing hydrogel of (a) 0.9 mg/mL thiolated gellan (G) and 12 mg/mL poly(MAM-co-MAA-co-BMAC) (CoP) represented as 0.9G_12CoP and (b) 1.5G_10CoP. At predetermined time intervals, the gel was dried and weighed. The percent degradation was determined by the given formula:

$$\text{Percentage mass loss} = \left(\frac{W_0 - W_t}{W_0} \right) * 100$$

where W_0 is the initial weight of the hydrogel and W_t is the weight of the gel at time t (days)

2.9. Isolation of Porcine Primary RPE

The procedures for extraction and passaging of primary porcine retinal pigment epithelial (ppRPE) cells were established similar to the protocol described by Toops et al. [21] with few modifications. The procured disinfected eye cups of pig eyes, after removal of the vitreous and retina, were incubated with 2 mL of 2× Trypsin with 5.3 mM EDTA in Hank's Balanced Salt Solution (HBSS) without Ca^{2+} and Mg^{2+} for 90 minutes. Cells were collected as per Toops protocol and plated at a density between 3000 to 4000 cells/cm². ppRPE cells were used at the first or second passage for this study.

2.10. *In vitro* Biocompatibility Test

Thiolated gellan was dissolved in sterile N₂-bubbled water and the poly(MAM-co-MAA-co-BMAC) was dissolved in sterile 2× Dulbecco's Modified Eagles' Medium/Nutrient Mixture F-12 Ham (DMEM/F12) media and the pH was adjusted to 7.4. 20% FCS, 2× penicillin/streptomycin, 2× gentamicin and 0.2× amphotericin were added to the copolymer to complete the 2× cell culture media. The thiolated gellan and poly(MAM-co-MAA-co-BMAC) solutions were then heated separately at 45 °C for 15 minutes and mixed immediately prior to application to the cells to obtain the composite solution. The solution was cast over the cells as described below.

The biocompatibility of hydrogel was tested using an ECIS (Applied BioPhysics, Troy, NY). Two sets of experiments were performed in this work. First, to determine the biocompatibility of a confluent layer of cells in contact with hydrogel, the ppRPE were plated at high cell density of 40,000 cells/well; ARPE-19 at 20,000 cells/well and 3T3/NIH (fibroblasts) cells at 10,000 cells/well. Epithelial cells were kept in culture for seven days to allow complete formation of tight junctions, while the fibroblasts were cultured for one day prior to addition of composite polymer solution. Due to the lack of contact inhibition in 3T3 cells, confluency was not reached till the end of the experiment. The cytotoxicity was interpreted as the decrease in resistance with respect to control and the effects on tight junctions were shown by changes in barrier resistance. These two characteristics were observed at an optimal frequency of 4,000Hz for six days after addition of polymer solution. In the second assay, the cells were plated at low density (ppRPE at 10,000 cells/well, ARPE-19 at 5,000 cells/well and 3T3/NIH at 4,000 cells /well), and the polymer solution was added the following day to investigate the proliferation of cells in the presence of gel. Simultaneously, the cell morphology was imaged using bright field microscopy on the 4th, 7th and 11th day after the addition of polymer solution. The cells were plated at the same density and time as the ECIS arrays in 96-well plates.

2.11 Animal study protocol and Vitrectomy

All studies are performed in accordance with the Association for Research in Vision and Ophthalmology (ARVO) resolution on the use of animals in vision and ophthalmic research. We perform the surgeries under general anesthesia and the rabbits are examined for a complete ophthalmic examination. After an established baseline conditions, a partial two–port pars plana vitrectomy is performed on the right eye of the rabbit. The left eye serves as the surgical control. Approximately 0.5 to 0.6 mL of vitreous from the temporal side of the cavity is removed using a 23 gauge vitrector (Pro Care Plus Vitrectomy System, Vision Care Devices, Redding, CA). This is followed by a fluid–air exchange and injection of approximately same volume of the polymer solution at 45 °C as the removed vitreous. The temperature of the polymer solution is reduced as it travels through the infusion line before reaching the vitreous cavity. However, the temperature of the polymer solution is above the Tgel and hence, in solution phase until gelling in the vitreous cavity. We perform detailed ophthalmic examinations involving an external and corneal examination, indirect ophthalmoscopy and intra-ocular pressure (IOP) measurement prior to surgery, on day 7 and 30 post-operation. Ocular coherence tomography (OCT) and fundus examinations are performed on rabbits 30 days after surgery. ERGs are performed prior to surgery and after 30 days. All rabbits are euthanized after the final examinations and the eye balls are procured for histology.

2.12. Statistical analysis

Results of hydrogel characterizations and surface model fittings designed from RSM were statistically analyzed using analysis of variance (ANOVA) with 95% confidence limits using Stat-Ease. All ECIS and biodegradation results are reported as mean \pm SD (standard deviation) (n = 3–4), where the error bars denote SD. In comparisons of the experimental groups to the control, F-test was performed to analyze the variance between the groups followed by a one-tail t-Test (assuming equal or unequal variances based on the result from

the F-test) with an alternative hypothesis of Mean(control) > Mean(experimental group). The experimental group is considered to be toxic to the cells if the t-Test is true. The p-value < 0.05 was considered to be statistically significant.

3. Results and Discussion

3.1 Polymer characterization

Thiol content and the polymer concentration of each component are the two important factors that have an impact on the hydrogel network architecture, rheological properties and biocompatibility. The thiol content of the thiolated gellan was found to be 11% (mol) of the repeat unit using NTSB assay. We noted that increasing the thiol content decreases the biocompatibility and the sol-gel transition temperature (results not shown). We determined that gellan with 11 mol % thiolation was optimal for this study. The thiol content of the poly(MAM-co-MAA-co-BMAC) copolymer was 2% (mol) from NTSB assay and ¹HNMR. Liang et al [17] showed that the poly(MAM-co-MAA-co-BMAC) with 2% (mol) thiol cross-linker and a methacrylate content of 20% (mol) was biocompatible on ocular epithelial cell lines.

Furthermore, this copolymer was well tolerated by ARPE-19 cells up to a concentration of 12.5 mg/mL, and at this concentration, increased % (mol) of thiol cross-linker was toxic to the cells. The concentration of thiolated gellan and poly(MAM-co-MAA-co-BMAC) was varied to generate series of hydrogels with tunable properties using a statistically designed RSM.

RSM is a statistical tool to determine the effects of the variables by performing minimum number of experiments. It can also be used to optimize the responses that are usually influenced by a number of important variables. In the D-optimal design algorithm, design points are optimally selected in the domain of interest that can deliver the maximum amount of information. In this study, the concentrations of each component are varied at five different levels and their influence on the physical, optical, mechanical, swelling and temperature transition properties of the hydrogel have been measured. The physical and optical properties of the hydrogels did not vary drastically with varying formulations. Refractive index measurements ranged from 1.334–1.338, density from 1.002–1.009 and the optical transmittance were greater than 85% in the visible wavelength. The optical transmittance in the ultraviolet range dropped drastically and was zero below 275 nm similar to that of the natural vitreous (Fig. A. 2). In contrast, the sol-gel transition temperature, storage and loss moduli, and swelling percentage varied with varying formulations of hydrogel as shown in Table 1.

3.2. Sol-gel Transition Temperature Characteristics of Hydrogel

Polymeric solution of formulation 0.9 mg/mL thiolated gellan (G) and 12 mg/mL poly(MAM-co-MAA-co-BMAC) (CoP), represented as 0.9G_12CoP, transitions to a gel at 40 °C (Fig. 2A) upon cooling from 55 °C. At a temperature above transition temperature (T_{gel}), the viscosity (loss moduli) of the material was larger than its elasticity (storage moduli) indicating that the solution phase was dominant over the gel phase and vice-versa,

at a temperature below Tgel, indicating the solid-like behavior of the material. Furthermore, the elastic physical gel, when oxidized with chemical crosslinks, is thermally irreversible and does not transition to a solution upon heating to higher temperature. The mixtures used in our work transition in the range of 35.5 to 42.5 °C (Table 1) depending on their formulation. The concentrations of both the components were statistically significant in governing the transition temperature of the hydrogel. Of the two, the concentration of thiolated gellan (p value <0.001) was more significant than copolymer (p value 0.0362) in the range of concentrations that we investigated. Thiolated gellan is essential for the temperature-triggered instantaneous physical gelation of the hydrogel, while varying the concentration of the copolymer helps in tuning to achieve desired Tgel. As the concentration of copolymer increases, the Tgel increases (Table 1, Fig. A. 3). The experimental data of hydrogels (Table 1) fits a cubic model according to the ANOVA with a p value of <0.0001 and a determination coefficient R² of 0.965; the equation is given below:

$$\begin{aligned} \text{Gelation temperature} = & 37.4 - 109.40 * [G] \\ & + 8.93 * [CoP] - 0.15 * [G] * [CoP] \\ & + 133.80 * [G]^2 \\ & - 0.93 * [CoP]^2 \\ & - 47.12 * [G]^3 + 0.03 * [CoP]^3 \end{aligned} \quad [1]$$

where 37.4 is the intercept of the data, [G] is the concentration of thiolated gellan in mg/mL and [CoP] is the concentration of copolymer in mg/mL.

3.3. Rheological Measurements of Hydrogel

The mechanical properties of the hydrogel, measured in terms of the storage modulus (G'; elastic or solid component) and the loss modulus (G''; viscous or liquid component) from the frequency sweep, depends on the concentration of the components of hydrogel. The storage modulus was greater than the loss modulus at all frequencies from 0.01 to 10 Hz for all formulations of hydrogel (Fig. 3A) indicating a gel-like behavior. The storage modulus of the swollen hydrogel ranged from 3.05 to 358 Pa while the loss modulus was 1.18 to 50.3 Pa at a frequency of 1Hz (Table 1). A linear regression model fits the experimental data for G' (Table 1) with a p value of <0.001 and R² of 0.795 from ANOVA. The linear surface of storage moduli with concentrations of thiolated gellan and copolymer is represented in Fig. 3B. The polynomial equation for this linear fit is given by

$$\text{Storage Moduli} = -141.60 + 150.97 * [G] + 10.73 * [CoP] \quad [2]$$

where -141.60 is the intercept of the model. We did not interpret for a negative value of the constant (intercept), as the model is not predicted at zero concentration of thiolated gellan and copolymer. The real value of this linear regression model is to understand how the storage moduli changes when we change the values of the variables ([G] and [CoP]).

Thiolated gellan (p value <0.0001) was found to be a more significant factor controlling the storage modulus than the copolymer (p value 0.001). The storage modulus of copolymer component without thiolated gellan was ~1.5 Pa at 0.9% (wt) [17]. However, with the addition of thiolated gellan, the storage modulus of a composite hydrogel of 1% (wt) copolymer and 0.05% (wt) thiolated gellan (Run #10, Table 1) was 35 Pa. Also, for a composite hydrogel of 1% (wt) copolymer and increasing concentrations of thiolated gellan (from 0.5 to 1.5 mg/mL), the G' increases from 35 Pa to 178 Pa. The thiolated gellan component contributes to the stiffness and rigidity to the hydrogel network.

3.4. Swelling Characteristics of Hydrogel

Our hydrogel swells in the presence of water or physiological fluid depending on the hydrogel composition. The swelling characteristics of our hydrogel are influenced by two different and opposite interactions. The ionic and flexible poly(MAM-co-MAA-co-BMAC) favors swelling in the presence of 1× PBS. The swelling capacity of the copolymer increases with the increase in MAA content and concentration (Fig. A.4). The MAA content of 20 % (mol) in our copolymer offers the maximum possible swelling [17]. On the other hand, thiolated gellan is a rigid component that forms a tight network that resists the swelling of the imbedded copolymer. Similar to this two-component system, in the natural vitreous, the innate need of HA to expand in physiological fluid, perhaps is counter-balanced by the collagen fibrillary mesh network, resulting in a tightly balanced network in swollen state. The swelling pressure offered by the tightly balanced vitreous within the cavity, along with its elastic response, may exert an osmotic pressure that can support the retina in its position.

The delta swelling of our hydrogels ranges from 0.38% to 27.81%. A linear regression model fits the swelling data of Table 1 with a p value of 0.0004 and R^2 of 0.676 from ANOVA. The delta swelling can be determined from the linear equation (3) where -10.31 is the intercept of the data, which is not interpreted as we do not calculate delta swelling for zero [G] and [CoP].

$$\text{Delta Swelling}[\%]= - 10.31+5.53 * [G]+1.80 * [CoP] \quad [3]$$

The concentration of copolymer (p value 0.0001) was relatively more significant than thiolated gellan (p value 0.1196) because thiolated gellan dampens the swelling capacity of the hydrogel. Hydrogel swelling within the vitreous cavity can be controlled such that it does not reach its equilibrium swelling and consequently produce swelling pressure and hence osmotic pressure to hold the retina in its position.

3.4. Optimization of Hydrogel

The formulations of hydrogel were optimized using numerical optimization in design-expert software for a transition temperature between 38–41 °C and storage moduli between 100–200 Pa. Transition temperature near physiological temperature is important for *in situ* forming hydrogels as the polymeric solution can be injected at a temperature that is slightly higher than the body temperature without causing heat-related trauma to the eye.

The mechanical properties of vitreous have been investigated by various groups as reviewed in detail by Swindle et al.[22]. The storage moduli of porcine vitreous from Nickerson et al. [2] is 10 ± 1.9 Pa and the bovine vitreous is 32 ± 12 Pa. However, the architecture of the natural vitreous changes when it is taken out of the vitreous cavity, which suggest that these values are lower than those found *in vivo*.

Furthermore, according to Zimmerlin et al. [23], the G' of bovine vitreous *ex vivo* with intact membrane is 120 Pa. G' of hydrogel is critical to withstand the saccadic movement of the eye; a quick movement of both the eyes that can vary from small amplitude with a frequency of $10^\circ/s$ to large amplitude with a frequency of $300^\circ/s$ [24]. The G' measurement at higher frequency mimics the situation for rapid eye movements. The G' of soft hydrogels like 0.5G_5CoP or 0.5G_10CoP, drops to 0 Pa at frequencies above 6.33 Hz. This implies that the polymeric material behaves like a liquid at high frequency which can cause a slippage between the cells and the polymer. Hence, to avoid the damage from impact and act as a shock absorber, storage moduli higher than 100 Pa would be suitable as vitreous substitute.

Consequently, three optimal formulations of composite hydrogel for specified Tgel and swollen storage moduli were chosen for further study. The formulations were 1.5G_5CoP, 0.9G_12 CoP and 1.5G_10CoP (Table 2). The sol-gel transition temperature, rheology and physical characteristics of the optimal formulations are tabulated (Table 2). All of the hydrogels were transparent to visible light, with density and refractive index similar to that of the natural vitreous. These formulations were further tested for *in vitro* biocompatibility and cell proliferation assay.

3.5. *In vitro* Biocompatibility and Proliferation Assay for Hydrogel

The biocompatibility of optimized formulations of hydrogel was analyzed using ECIS. ECIS is a noninvasive technique that measures the impedance across gold electrodes present in the bottom of tissue culture wells from 400 to 64000 Hz frequencies of alternating current. In cytotoxicity assay, cells were plated in wells containing gold electrodes and the resistance at various frequencies changes with the change in cell morphology and attachment to the electrodes. The addition of polymer gel on the electrodes further complicates the impedance of the system. Therefore, for our study, the resistance of the cell-gel system was monitored over time at a 4,000 Hz as the contribution of resistance from cells was dominant over the contribution of resistance from hydrogel with media.

The epithelial and fibroblastic cell lines are biocompatible with the optimized formulations of the hydrogels (Fig. 4). ARPE-19 cells revealed no significant change in resistance or toxicity (failed t-Test) compared to control cells in the presence of the three hydrogels for six days (Fig. 4A). The control is the resistance of cells without the addition of the gel. The resistance peaks on the third and fifth day were due to the addition or change of the media. This was mainly to allow the diffusion of nutrients present in the media through the hydrogel to reach the confluent layer of cells and mimic the natural eye conditions. The 3T3/NIH fibroblast cells show no toxicity (failed t-Test, $p > 0.05$) similar to ARPE-19 cells (Fig. 4C). The ppRPE cells show no toxicity with the hydrogel of formulation 1.5G_5CoP (Fig. 4B).

However, the resistance of ppRPE cells in contact with the other two formulations show a 30% decrease for the first three days (Fig. 4B). The cells do recover within the next two days and achieve the same resistance as the control at the end of six days. The initial decrease in resistance may correspond to the presence of thiol groups in the physical gel in contact with the cells. The thiol groups takes a maximum of three days [17] for complete oxidation to form disulfide linkages in the hydrogel. In the first three days, the cells compete with the thiol groups for dissolved oxygen. Upon addition of fresh media on the third day, the cells recovered quickly. In addition, the t-Test on the ppRPE cells in contact with the hydrogels on day 6 failed statistically, and revealed that the cells are biocompatible with all the three hydrogels.

The cells in growth-phase or in proliferation are also biocompatible with our hydrogels (Fig. 4D, E &F). The resistance peaks at various times indicate the aspiration and addition of new media. The cell morphology was also followed after addition of the polymer solution. Fig. 5 shows cells in contact with the formulation 0.9G_12CoP observed under bright field microscope at 10× magnification on day 4, 7 and 11 after the addition of polymer solution. Both the ARPE-19 and ppRPE cells proliferate well in the presence of all the three optimized formulations of hydrogel (Fig. 4D &E). The resistance of the cells after 10 days in contact with gel was significantly higher compared to the control cells without the gel (p-value <0.01, failed t-Test). With the ppRPE there is an initial drop in resistance, which did not affect the growth of cells (Fig. 4E). The morphology for the retinal cells was not affected by any formulation and the images show that the number of cells increased with time (Fig. 5). These findings indicate (1) the three formulations are biocompatible with the ppRPE and ARPE-19 cell lines and (2) the studies of hydrogel obtained from ECIS are consistent with changes in cell morphology. 3T3/NIH cells also proliferated in the presence of the three hydrogel formulations (Fig. 4F). The cells in contact with the 1.5G_5CoP hydrogel statistically failed the t-Test on day 5 and with other two hydrogels on day 6; however after day 7, cell growth and activity was lower than that the control cells. The bright field microscopic images of 3T3/NIH cells indicated that there may be a slight slowing of cell growth in contact with 0.9G_12CoP hydrogel by day11 (Fig. 5). However, the morphology of the 3T3/NIH cells still appeared to be relatively normal.

The barrier resistance (R_b) of the three cell lines was analyzed by software modeling, which separates out the different components of cell-layer resistance, to check if the hydrogel affects the integrity of the cell junctions. The barrier resistance of ARPE-19 and 3T3/NIH cells was not affected by the three hydrogels and they followed a similar pattern as the resistance measured in fig. 4A, C (results not shown). In Fig. 6, the R_b was shown from the time of the plating of the ppRPE cells. After complete tight junction formation, the R_b was around 3.25 – 3.75 times the resistance of the empty well. The control ppRPE cell barrier functions started to deteriorate from day 7 on. After the addition of polymer, the barrier resistance for ppRPE was lower than the controls from day 1 to 3, similar to results observed at 4,000Hz. However, with the formation of the permanent gel and media change, the R_b recovered significantly and also failed the t-Test on day 12, indicating that the tight junctions of the cells reformed (Fig. 6). Preliminary *in-vivo* studies in rabbits with 0.9G_12CoP hydrogel have not shown any apparent adverse effects on the retinal structures by optical coherence tomography (OCT) and direct retinal visualization by a vitreo-retinal surgeon

(Fig. 7) thus far. The vitreous remained optically clear and revealed no retinal detachment or atrophy in retinal thickness. Also, IOP was not raised by the gel. Ongoing studies are underway to investigate the biocompatibility and degradation of hydrogel in a rabbit model.

3.6. *In vitro* Degradation of Hydrogel

Our hydrogel did not show significant loss in mass (p value > 0.05) in the presence of lysozyme and trypsin for four weeks. In fact, a slight increase in mass was observed similar to the control (Fig. 8A). Slight increase in mass might be due to swelling and protein absorption in our hydrogels in contact with the enzymatic solutions. The storage moduli of 0.9G_12CoP and 1.5G_10CoP hydrogels incubated with enzymatic solutions traced similar pattern as the control after four weeks (Fig. 8B). We chose lysozyme and trypsin for our degradation studies as lysosomal enzymes are distributed widely in various ocular tissue and trypsin is a commonly used enzyme in degradation studies that hydrolyzes proteins. Van deemter et al [25] detected the presence of trypsin in the vitreous, and its function in degradation of collagen fibrils. Our hydrogels did not degrade over a 28 days due to the strong chemical cross-links (S-S linkages) in the hydrogel network.

4. Conclusions

We have designed a potentially reversible *in situ* forming two-component hydrogel with thiolated gellan and a poly(MAM-co-MAA-co-BMAC) copolymer that can mimic the natural vitreous. The physical, mechanical and the optical properties of our hydrogels are close to those of the natural vitreous. In addition, our hydrogels transition rapidly from liquid to gel near physiological temperature, which should physically trap the copolymer, preventing diffusion before the formation of disulfide bonds. It swells in physiological fluid to produce osmotic pressure to keep the retina in its position. The mechanical property, transition temperature, and extent of swelling of our hydrogel can be adjusted by changing the concentration of each component. Although both the components are significant in controlling the properties, concentration of the thiolated gellan is statistically more significant than that of the copolymer in controlling the storage modulus and transition temperature, while the concentration of copolymer is critical in governing the extent of swelling. From the observation of bio-mimetic hydrogel, perhaps, the collagen scaffold controls the stiffness of the vitreous and also resists the swelling of HA. The swelling force of HA and the resistive force of collagen against it may control the swelling pressure of vitreous and hence, the osmotic pressure to keep the retina in place. The three optimized hydrogels, 0.5G_10CoP, 0.9G_12 CoP and 1.5G_10CoP, have properties close to natural vitreous, and were biocompatible *in vitro* with ppRPE, ARPE-19 and fibroblast 3T3/NIH cells. The hydrogels did not impair tight junction formation or affect proliferation. Preliminary rabbit studies on 0.9G_12CoP have not revealed any adverse effects on the retinal structure or function. Furthermore, our hydrogel did not degrade *in vitro* for about four weeks and can be recommended for further testing *in vivo* as a long-term vitreous substitute.

Supplementary Material

Refer to Web version on PubMed Central for supplementary material.

Acknowledgments

This research was supported by an NIH grant, EY021620 and a Department of Veterans Affairs rehab merit review grant RX000657-01 to Dr. Nathan Ravi. Also, Research to Prevent Blindness, Inc. and NIH Core Grant P30 EY02687 provided support.

References

1. Gloor, BP. The Vitreous. In: Moses, RA., Hart, WM., editors. *Adler's Physiology of the Eye-Clinical Application*. The CV Mosby Co; St Louis: 1987. p. 246-267.
2. Nickerson CS, Karageozian HL, Park J, Kornfield JA. Internal tension: A novel hypothesis concerning the mechanical properties of the vitreous humor. *Macromolecular Symposia*. 2005; 227:183–189.
3. Lee B, Litt M, Buchsbaum G. Rheology of the vitreous body. Part I: Viscoelasticity of human vitreous. *Biorheology*. 1992; 29(5-6):521–33. [PubMed: 1306380]
4. Baino F. Towards an ideal biomaterial for vitreous replacement: Historical overview and future trends. *Acta Biomater*. 2011; 7(3):921–35. [PubMed: 21050899]
5. Pastor JC, Lopez MI, Saornil MA, Refojo MF. Intravitreal silicone and fluorosilicone oils-pathological findings in rabbit eyes. *Acta Ophthalmologica*. 1992; 70(5):651–658. [PubMed: 1471491]
6. Pastor Jimeno JC, de la Rua ER, Fernandez Martinez I, Nalda MJ del Nozal, Jonas JB. Lipophilic substances in intraocular silicone oil. *American journal of ophthalmology*. 2007; 143(4):707–9. [PubMed: 17386289]
7. Federman JL, Schubert HD. Complications associated with the use of silicone oil in 150 eyes after retina-vitreous surgery. *Ophthalmology*. 1988; 95(7):870–876. [PubMed: 3174036]
8. Suri S, Banerjee R. In vitro evaluation of in situ gels as short term vitreous substitutes. *J Biomed Mater Res A*. 2006; 79(3):650–64. [PubMed: 16826595]
9. Su WY, Chen KH, Chen YC, Lee YH, Tseng CL, Lin FH. An injectable oxidated hyaluronic acid/adipic acid dihydrazide hydrogel as a vitreous substitute. *J Biomater Sci Polym Ed*. 2011; 22(13):1777–97. [PubMed: 20843434]
10. Tortora M, Cavalieri F, Chiessi E, Paradossi G. Michael-type addition reactions for the in situ formation of poly(vinyl alcohol)-based hydrogels. *Biomacromolecules*. 2007; 8(1):209–214. [PubMed: 17206809]
11. Annaka M, Mortensen K, Vigild ME, Matsuura T, Tsuji S, Ueda T, Tsujinaka H. Design of an injectable in situ gelation biomaterials for vitreous substitute. *Biomacromolecules*. 2011; 12:4011–21. [PubMed: 21988210]
12. Chang J, Tao Y, Wang B, Guo B-h, Xu H, Jiang Y-r, Huang Y. An in situ-forming zwitterionic hydrogel as vitreous substitute. *Journal of Materials Chemistry B*. 2015; 3(6):1097–1105.
13. Tao Y, Tong X, Zhang Y, Lai J, Huang Y, Jiang YR, Guo BH. Evaluation of an in situ chemically crosslinked hydrogel as a long-term vitreous substitute material. *Acta Biomater*. 2013; 9(2):5022–30. [PubMed: 23022890]
14. Foster WJ, Aliyar HA, Hamilton P, Ravi N. Internal osmotic pressure as a mechanism of retinal attachment in a vitreous substitute. *Journal of Bioactive and Compatible Polymers*. 2006; 21(3):221–235.
15. Swindle-Reilly KE, Shah M, Hamilton PD, Eskin TA, Kaushal S, Ravi N. Rabbit study of an in situ forming hydrogel vitreous substitute. *Invest Ophthalmol Vis Sci*. 2009; 50(10):4840–6. [PubMed: 19324846]
16. Rozier A, Mazuel C, Grove J, Plazonnet B. Functionality testing of gellan gum, a polymeric excipient material for ophthalmic dosage forms. *International Journal of Pharmaceutics*. 1997; 153(2):191–198.
17. Liang J, Struckhoff J, Du H, Hamilton P, Ravi N. Synthesis and Characterization of In Situ Forming Anionic Hydrogel as Vitreous Substitute. *Journal of Biomedical Materials Research Part B*. in press.

18. Nakagawa M, Tanaka M, Miyata T. Evaluation of collagen gel and hyaluronic acid as vitreous substitutes. *Ophthalmic Research*. 1997; 29(6):409–420. [PubMed: 9380343]
19. Thannhauser TW, Konishi Y, Scheraga HA. Analysis for disulfide bonds in peptides and proteins. *Methods Enzymol*. 1987; 143:115–9. [PubMed: 3657523]
20. Du H, Hamilton P, Reilly M, Ravi N. Injectable in situ physically and chemically crosslinkable gellan hydrogel. *Macromol Biosci*. 2012; 12(7):952–61. [PubMed: 22707249]
21. Toops KA, Tan LX, Lakkaraju A. A detailed three-step protocol for live imaging of intracellular traffic in polarized primary porcine RPE monolayers. *Exp Eye Res*. 2014; 124:74–85. [PubMed: 24861273]
22. Swindle-Reilly, K., Ravi, N. Designing hydrogels as vitreous substitutes in ophthalmic surgery. In: Charila, T., editor. *Biomaterials and Regenerative Medicine in Ophthalmology*. Woodhead Publishing Ltd., CRC Press; 2010. p. 339-373.
23. Zimmerlin JA, McManus JJ, Crosby AJ. Cavitation rheology of the vitreous: mechanical properties of biological tissue. *Soft Matter*. 2010; 6(15):3632–3635.
24. Piccirelli M, Bergamin O, Landau K, Boesiger P, Luechinger R. Vitreous deformation during eye movement. *Nmr in Biomedicine*. 2012; 25(1):59–66. [PubMed: 21567512]
25. van Deemter M, Kuijter R, Pas HH, van der Worp RJ, Hooymans JMM, Los LI. Trypsin-mediated enzymatic degradation of type II collagen in the human vitreous. *Molecular Vision*. 2013; 19:1591–1599. [PubMed: 23882137]

Statement of Significance

Although hydrogels are researched as long-term vitreous substitute, none have advanced sufficiently to reach clinical application. Our work focuses on the development of a novel two-component *in situ* forming hydrogel that bio-mimic the natural vitreous. Our thiol-containing copolymers can be injected as an aqueous solution into the vitreous cavity wherein, at physiological temperature, the rigid component will instantaneously form a physical gel imbedding the random coil copolymer. Upon subsequent oxidation, the two components will form disulfide cross-links and a stable reversible hydrogel capable of providing osmotic pressure to reattach the retina. It may be left in the eye permanently or easily removed by injection of a simple reducing agent to cleave the disulfide bonds, rather than surgery. This contribution is significant because it is expected to provide patients with a much better quality of life by improving surgical outcomes, creating much less post-operative burden, and reducing the need for secondary surgeries.

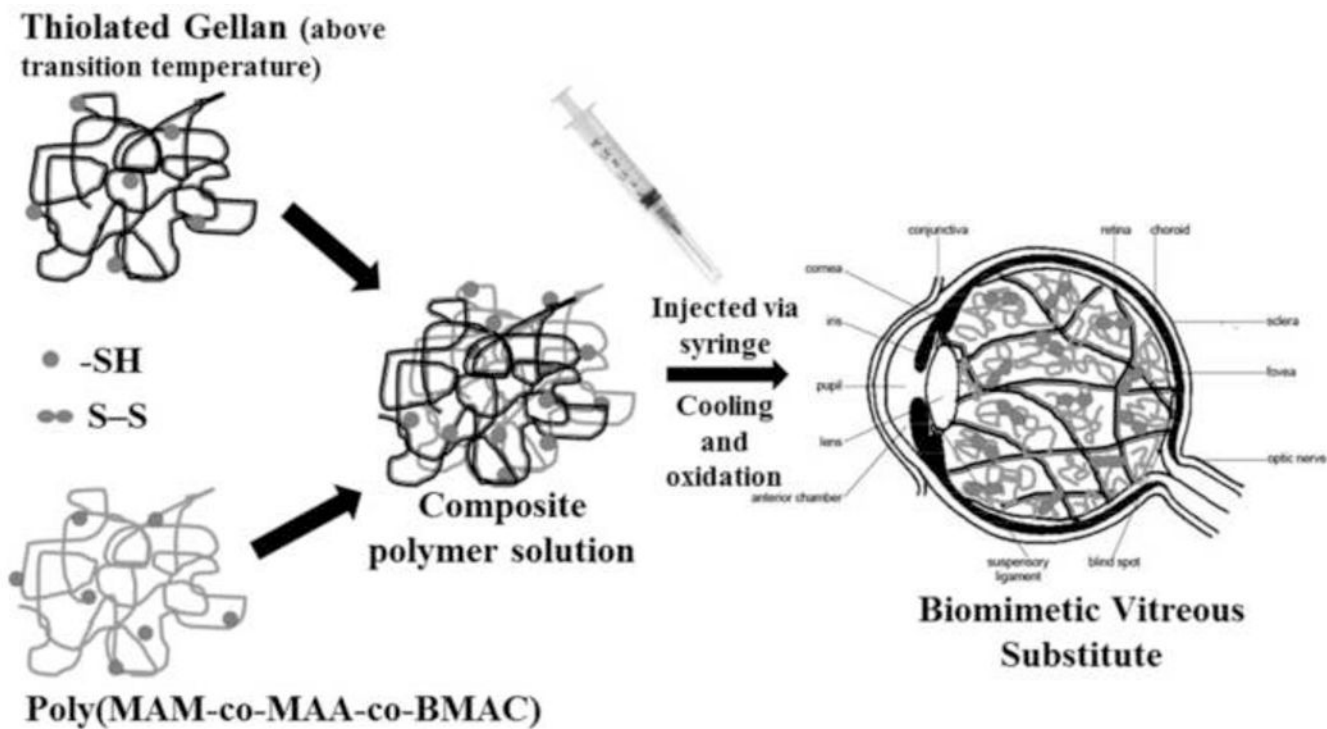


Fig. 1. Schematic representation of our two-component polymer solution injected via syringe into the vitreous cavity, which forms an instantaneous physically crosslinked hydrogel upon cooling and a chemically crosslinked network with established disulfide bonds on oxidation.

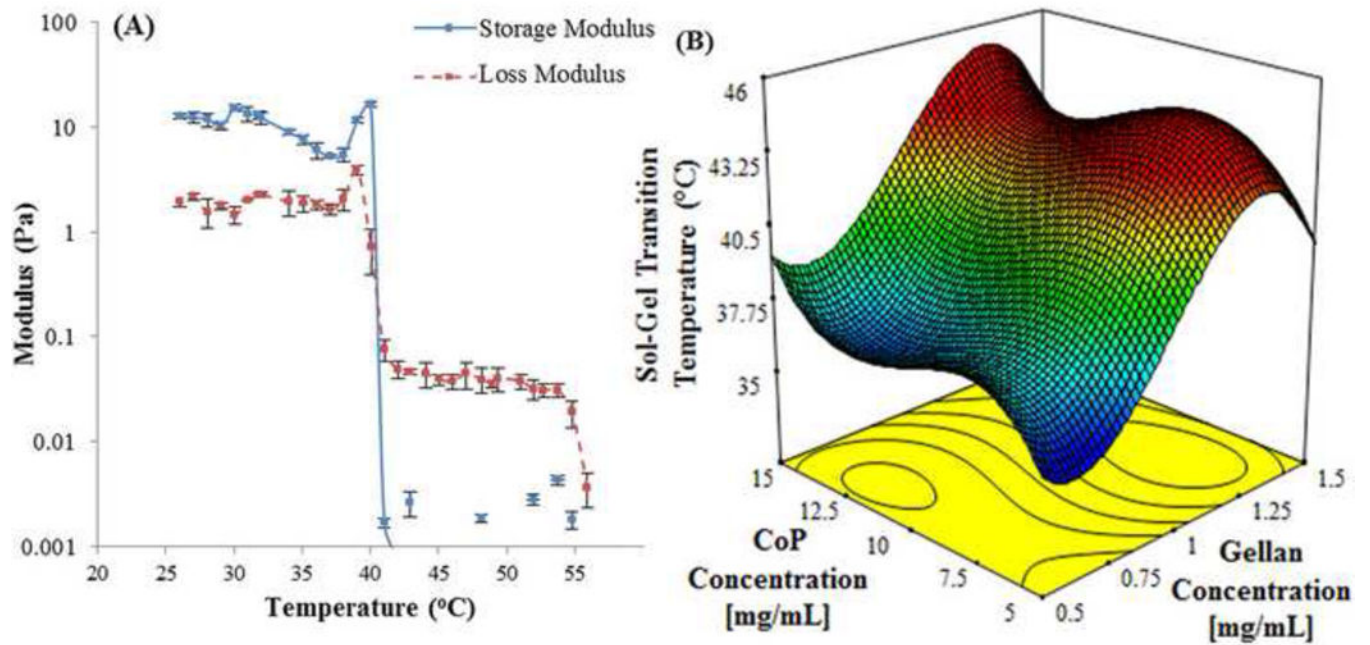


Fig. 2. (A) Temperature scans for a mixture of 0.9 mg/mL thiolated gellan and 12 mg/mL poly(MAM-co-MAA-co-BMAC). (B) A modelled cubic surface plot of sol-gel transition temperature against concentration of thiolated gellan and copolymer in mg/mL.  represents the gradient of colors with increasing transition temperature from 35.5 to 43 °C.

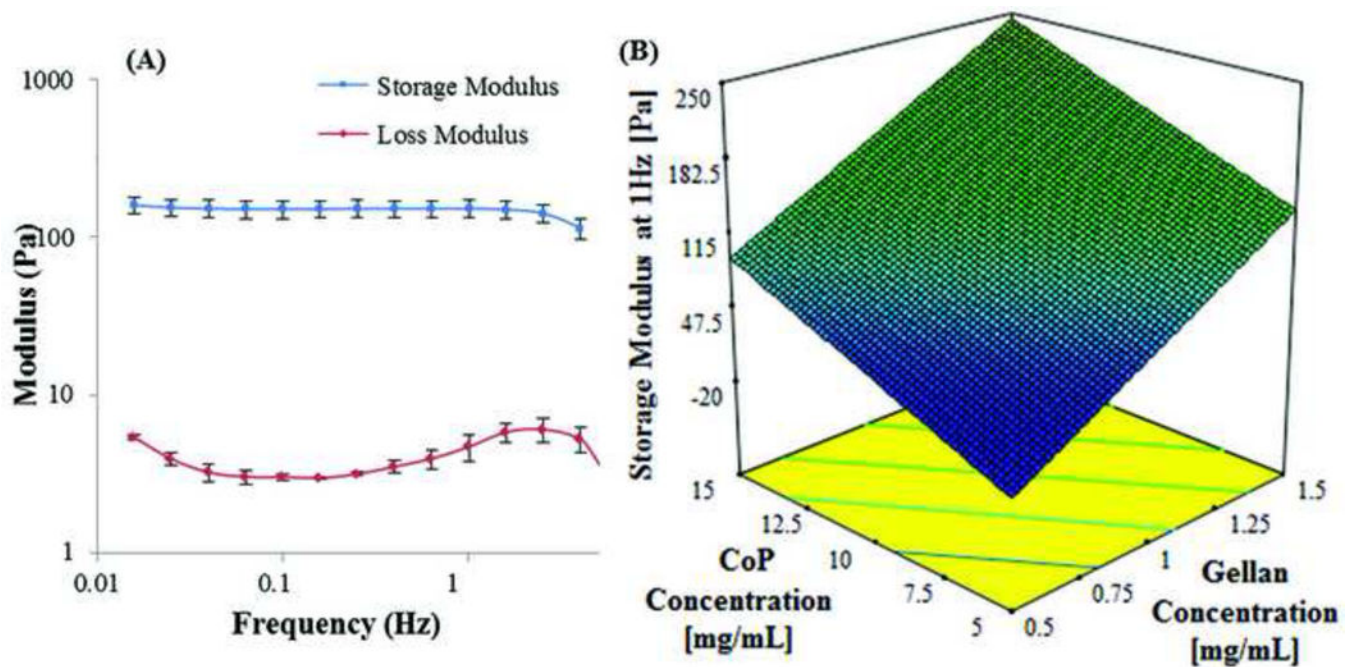


Fig. 3.

(A) Storage and loss modulus of composite hydrogel of formulation 0.9 mg/mL thiolated gellan and 12 mg/mL poly(MAM-co-MAA-co-BMAC). (B) A modelled surface plot of storage modulus in Pa at 1 Hz against change in concentration of thiolated gellan and copolymer (CoP) in mg/mL. The modelled data is based on storage modulus results from 17 composite hydrogel. The results fit the modelled surface with a p value of <0.001 obtained from ANOVA.  represents the gradient of colors with increasing storage modulus from 3 to 358 Pa.

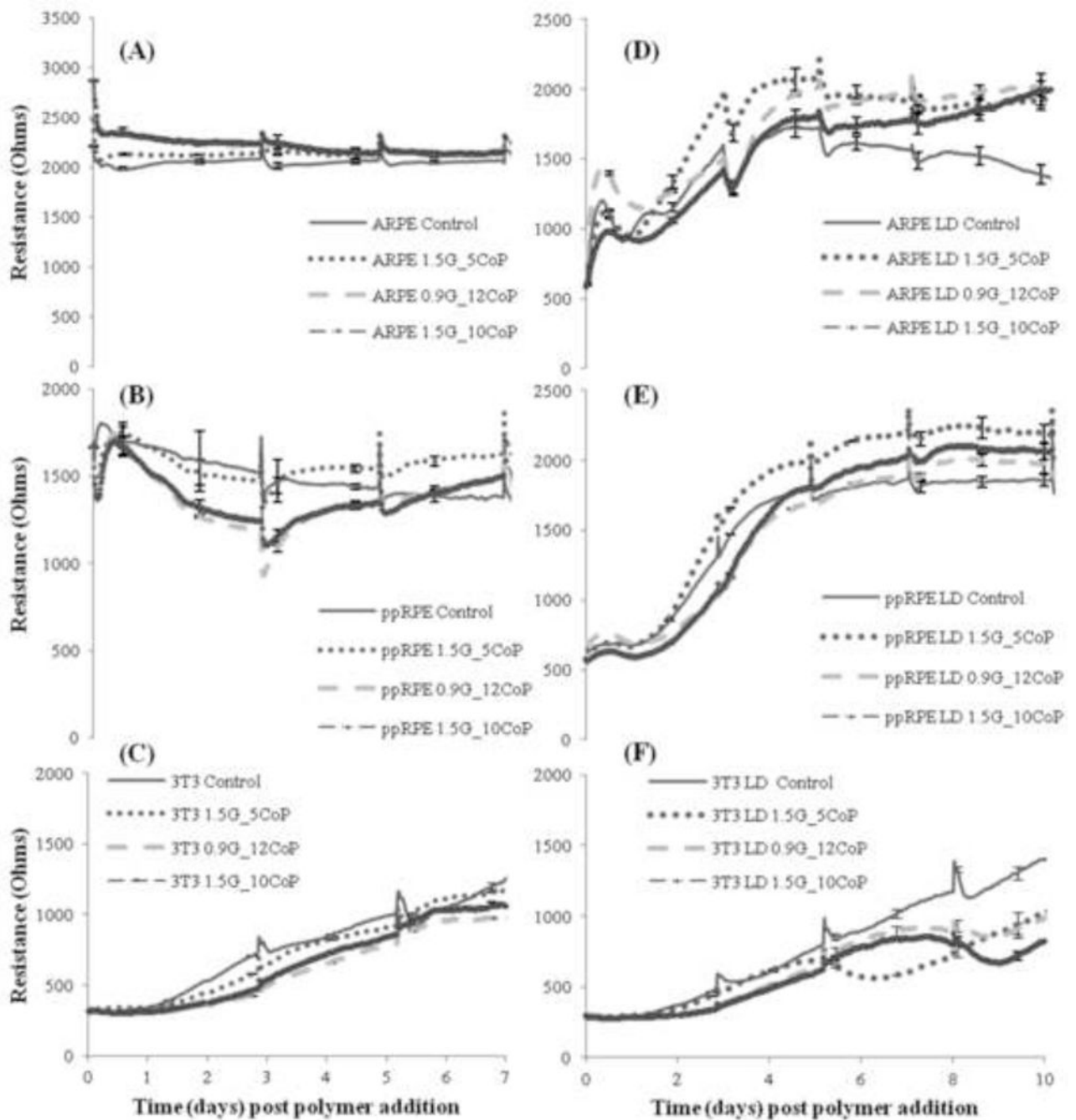


Fig. 4. Tracings show measured resistance of the cells in contact with three different formulations hydrogel with time post polymer (hydrogel) addition. Control is cells without hydrogel. The 4,000Hz is the optimal frequency for measuring the biocompatibility of the cells at either high density (non-proliferative, Fig A,B,C) or low density (proliferative, Fig D,E,F) conditions. Each data point represents the average of four wells and error bars represent standard error given by standard deviation over square root of the well number. The individual cell lines are ARPE, ppRPE and 3T3 as mentioned in the Fig. legends.

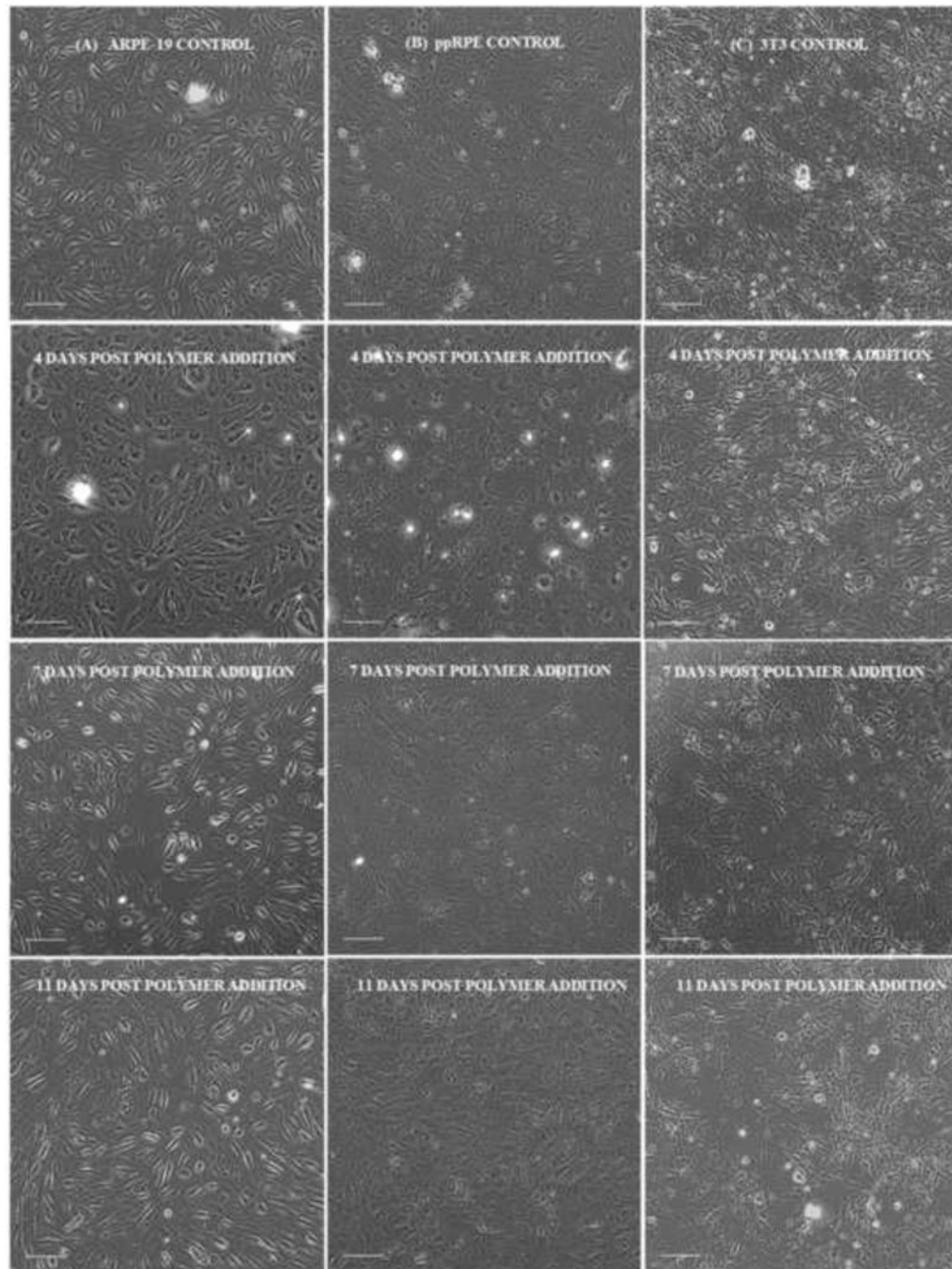


Fig. 5. Bright field image of (A) ARPE-19 (B) ppRPE and (C) 3T3/NIH cells alone (control on 11th day) and cells in contact with composite hydrogel 0.9G_12CoP on 4th, 7th and 11th day (column wise) post polymer addition (Scale bar – 100 μ m).

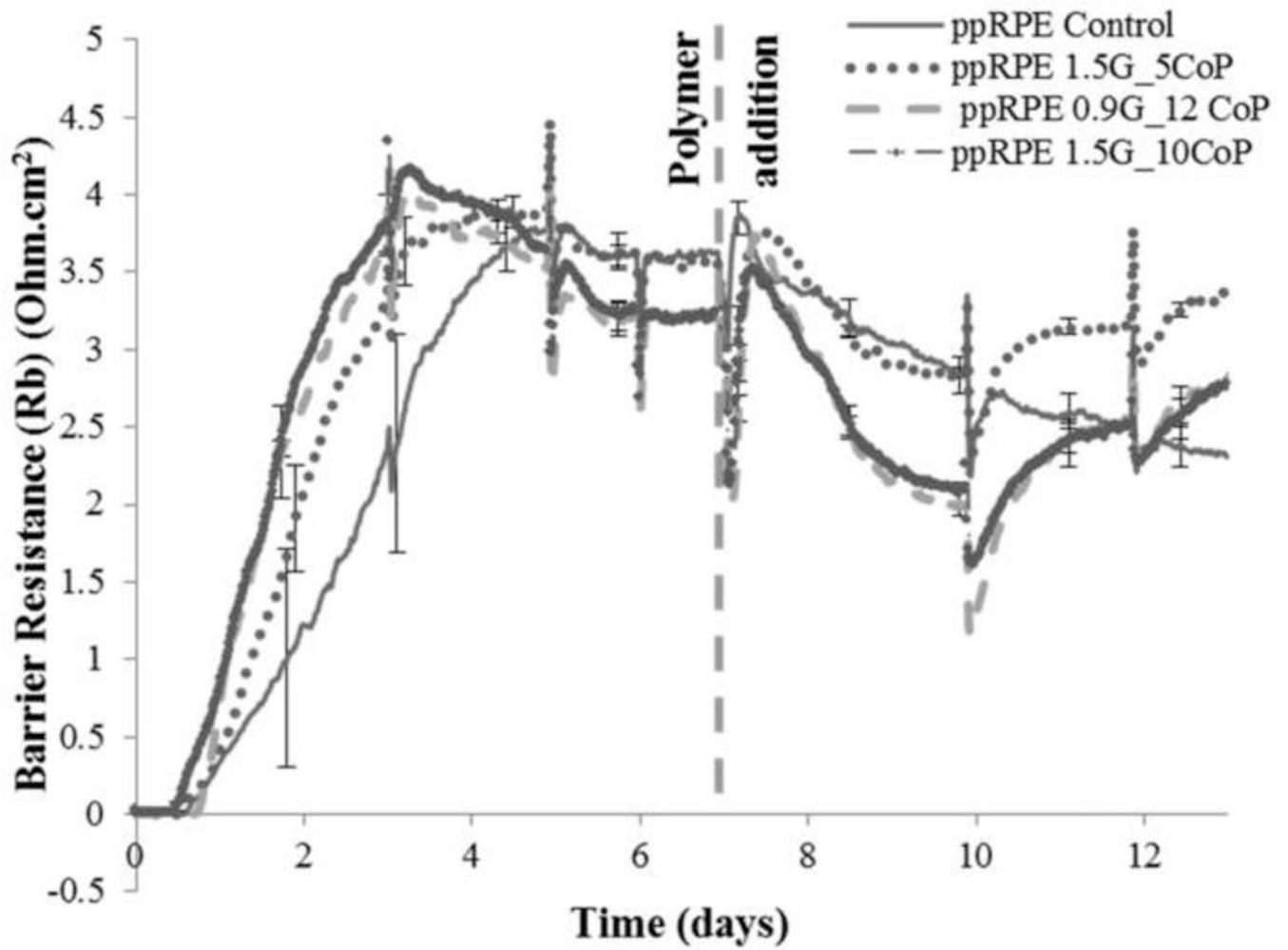


Fig. 6. Barrier resistance (R_b) measurements in Ohm.cm^2 at a frequency of 400 Hz over time (days) post polymer addition for ppRPE cells plated at high density (40,000 cells/well) for three different formulations of hydrogel.

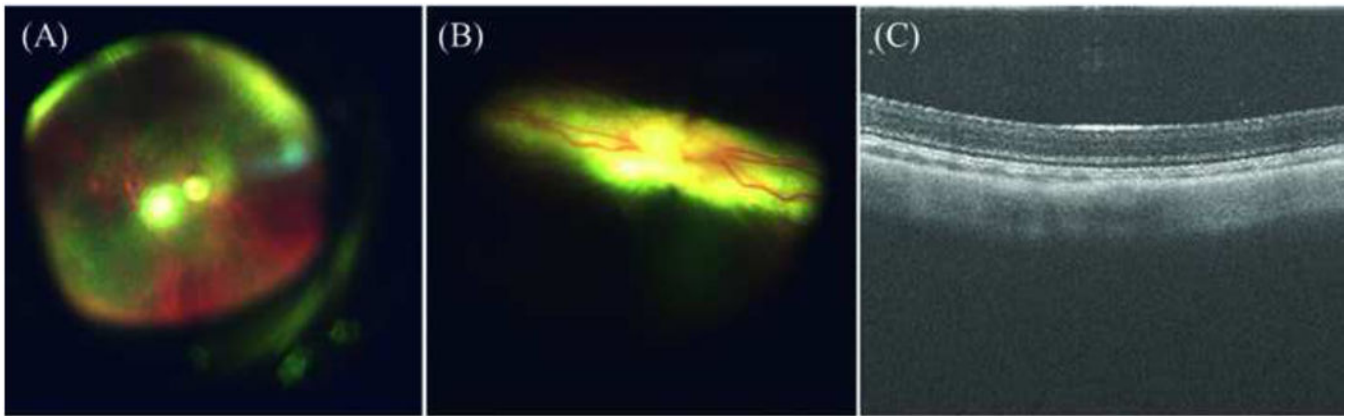


Fig. 7. Direct visualizations (Fundoscopy) and optical coherence tomography (OCT) of rabbit retina. (A) Fundoscopic image of rabbit choroid which underwent partial vitrectomy and replaced with our bio-mimetic hydrogel of formulation 0.9 mg/mL gellan and 12 mg/mL copolymer after 4 weeks duration. (B) Fundoscopic image of rabbit retina with our bio-mimetic vitreous substitute after 4 weeks and (C) The cross-section of rabbit retina in contact with hydrogel after 4 weeks using OCT. The vitreous remained optically clear and revealed no retinal detachment or atrophy in retinal thickness.

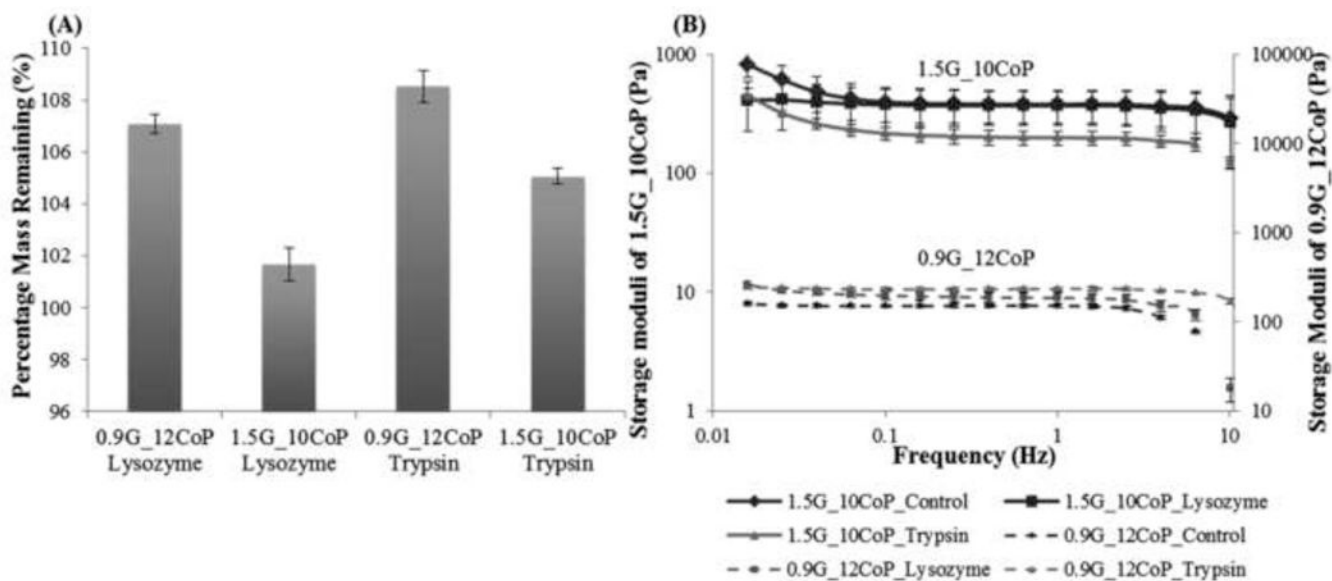


Fig. 8. Degradation studies. (A) Percentage of mass remaining in the hydrogels 0.9G_12CoP and 1.5G_10CoP after 4 weeks in the presence of lysozyme and trypsin. (B) Storage moduli of 1.5G_10CoP and 0.9G_12CoP at different frequencies. Control is the hydrogel in 1× PBS. Storage moduli of 1.5G_10CoP is plotted in primary axis while 0.9G_12CoP in secondary axis. Error bars are the standard deviation from three replicates of each sample.

Table 1
Sol-gel transition temperature, storage and loss moduli, and percentage swelling for 17 hydrogel designed from RSM

Run Number with run number of replicates given in brackets	Gellan Concentration [mg/mL]	CoP Concentration [mg/mL]	Sol-gel transition temperature [°C]	Storage Modulus at 1 Hz [Pa] Swollen state	Loss Modulus at 1 Hz [Pa] Swollen state	Delta Swelling [%]	Weight Percent of dried polymer in equilibrium swollen hydrogel [%]
1	0.75	12.5	37.0	51.3	3.12	3.67	1.28
2	1	10	41.5	106	4.55	22.28	0.90
3	1.5	15	42.5	358	50.30	20.98	1.36
4	1.5	10	41.5	178	7.48	13.35	1.01
5	1.5	5	39.5	151	12.00	6.37	0.58
6 (3)	1.5	15	41.8	199	10.20	27.81	1.29
7 (2)	1	10	40.8	115	13.90	5.78	1.04
8 (5)	1.5	5	40.0	138	3.82	4.82	0.62
9	1	7.5	41.8	67.7	4.47	7.07	0.79
10	0.5	10	36.8	35.1	4.45	10.74	0.95
11	0.5	5	35.5	3.05	1.18	1.67	0.54
12	0.5	15	40.5	113	38.80	23.47	1.26
13	1	15	42.5	143	7.70	24.11	1.29
14	1.25	12.5	43.0	173	8.52	19.70	1.15
15 (2)	1	10	41.5	91.8	5.02	17.27	0.94
16 (11)	0.5	5	36.0	21.1	3.35	0.38	0.55
17 (12)	0.5	15	38.8	120	28.70	22.03	1.27

Table 2 Rheological and physical properties of composite hydrogel of three optimized formulations from RSM

Formulation	Thiolated gellan Concentration [mg/mL]	CoP Concentration [mg/mL]	Sol-gel transition temperature [°C]	Swollen Storage Modulus at 1 Hz [Pa]	Swollen Loss Modulus at 1 Hz [Pa]	Refractive Index	Density	Average Light transmittance (%) from 400–800 nm
1.5G_5CoP	1.5	5	39.75	144.5	7.91	1.3351	1.009	93.6
0.9G_12 CoP	0.9	12	40.2	151	4.73	1.3355	1.003	94
1.5G_10 CoP	1.5	10	41.5	178	7.48	1.3372	1.006	87.6